A Minimum Model Error Approach for Attitude Estimation

John L. Crassidis
NRC Resident Research Fellow, Member AIAA
Goddard Space Flight Center, Code 712
Greenbelt, MD 20771

F. Landis Markley
Staff Engineer, Associate Fellow AIAA
Goddard Space Flight Center, Code 712
Greenbelt, MD 20771

Abstract

In this paper, an optimal batch estimator and filter based on the Minimum Model Error (MME) approach is developed for three-axis stabilized spacecraft. This robust algorithm accurately estimates the attitude of a spacecraft with or without the utilization of angular rate measurements from gyros. The absence of rate data may be a result of intentional design or from unexpected failure of existing gyros. The formulation described in this paper is shown using only attitude sensors (e.g., three-axis magnetometers, sun sensors, star trackers, etc). The functional form of the optimal estimation approach involves a gradient search and a linearization technique with a linear Riccati transformation. This algorithm is computationally efficient and provides accurate state estimates. Results using this new algorithm indicate that an MME-based approach accurately estimates the attitude of an actual spacecraft with the use of only magnetometer sensor measurements.

Introduction

The attitude of a spacecraft can be determined by either deterministic methods or by utilizing algorithms which combine dynamical models with sensor data. Three-axis deterministic methods, such as TRIAD [1], QUEST [2], and FOAM [3], require at least two sets of vector measurements to determine the attitude (direction-cosine) matrix. An advantage of both the QUEST and FOAM algorithms is that the attitude of a spacecraft can be estimated using more than two sets of measurements. This is accomplished by minimizing a quadratic loss function first posed by Wahba [4]. However, all deterministic methods fail when only one set of vector measurements is available, (e.g., magnetometer data only). Estimation algorithms utilize dynamic models and subsequently can (in theory) estimate the attitude of a spacecraft using only one set of vector measurements. Although all spacecraft in use today have at least two on-board attitude sensors, estimation techniques can be used to determine the attitude during anomalous periods, such as solar eclipse and/or sensor co-alignment.

The most commonly used technique for attitude estimation is the Kalman filter [5]. The Kalman filter utilizes state-space representations to both estimate plant dynamics and also filter noisy data. Errors in the dynamical model and measurement process are assumed to be modeled by a zero-mean Gaussian process with known covariance. The optimality criterion in the Kalman filter minimizes the trace error covariance between estimated responses and model responses. In theory, the Kalman filter does not require actual measurements to satisfy this optimality criterion; however, in actual practice measurements are often used to properly "tune" the filter estimates.

Smoothing algorithms further refine state estimates by utilizing both a "forward filter" and a "backward filter" (see e.g., Gelb [6]). An advantage of smoothing algorithms is that the error covariance is always less or equal to either the forward or backward filter alone. A disadvantage of smoothing algorithms is that they cannot be implemented in sequential (real-time) estimation.

Early practical applications of Kalman filtering for attitude estimation are given by Pauling et al. [7] and Toda et al. [8], for the Space Precision Attitude Reference System (SPARS). In particular, Pauling et al. [7] used the now familiar quaternion representation for model prediction in the filter design. Since, the quaternion representation is free of singularities (thus avoiding the "gimbal-lock" situation), and since the attitude matrix is algebraic in the quaternion components, this representation is most frequently used in attitude determination and estimation algorithms. A more complete survey of other attitude representations is given by Shuster [9]. Also, a more complete survey of early Kalman filtering techniques for attitude estimation is given by Lefferts et al [10].

Recent studies using Kalman filtering techniques have been performed for the Earth Radiation Budget Satellite (ERBS) [11-12], the Upper Atmospheric Research Satellite (UARS) [13], the Extreme Ultra Violet Explorer (EUVE)

[14], and the Solar Anomalous Magnetospheric Particle Explorer (SAMPEX) [15-16]. In particular, studies of the EUVE spacecraft involved the application of a smoothing algorithm to further reduce errors in the estimated attitudes using both attitude sensors and gyro data. Also, studies of both the ERBS and SAMPEX spacecraft used Kalman filtering techniques for attitude estimation which involved gyro degradation or gyro omission. The thrust of all of these investigations is to improve attitude estimates through the use of optimally tuned filter parameters, thereby providing the means for reliable backup attitude estimation schemes.

In order for the Kalman filter to be truly optimal, both the measurement error process and model error process must be random Gaussian processes with known covariance. In most circumstances, properties of the measurement error process are known a priori by utilizing statistical inferences applied to sensor measurements. However, model error statistics are not usually well known. In actual practice the determination of the model error covariance in the Kalman filter is usually obtained by an ad hoc and/or heuristic approach, which can result in suboptimal filter designs (e.g., determining random gyro drift rate). Also, in many instances, such as nonlinear model errors or non-stationary processes, the assumption of a stationary Gaussian process can lead to severely degraded state estimates.

For spacecraft attitude estimation, the Kalman filter is most applicable to spacecraft equipped with three-axis gyros as well as attitude sensors [10]. However, rate gyros are generally expensive and are often prone to degradation or failure. Therefore, in recent years rate gyros have been omitted (e.g., in Small Explorer (SMEX) spacecraft, such as SAMPEX). To circumvent the problem of rate gyro omission or failure, analytical models of rate motion can be used. This approach has been successfully used in a Real-Time Sequential Filter (RTSF) algorithm which propagates state estimates and error covariances using dynamic models (see [16]). The estimation of dynamic rates by the RTSF is accomplished from angular momentum model propagation, and then correcting for these rates by using a "gyro bias" component in the filter design. A clear advantage of using dynamic models is shown for the case of near co-alignment of the spacecraft-to-sun and magnetic field vectors. For this case, deterministic algorithms, such as TRIAD and QUEST, show anomalous behaviors with extreme deviations in determined attitudes. Since the RTSF propagates an analytical model of motion, attitude estimates are improved even when data from only one attitude sensor is available. However, the RTSF is essentially a Kalman filter in which the "gyro bias" model (and subsequently the angular momentum model correction) is assumed to be a Gaussian process with known covariance. Also, fairly accurate models of angular momentum are required in order to obtain accurate estimates. Subsequently, the design process for choosing the model error covariance becomes difficult.

Other approaches to using a Kalman filter with no gyro data are discussed by Chu and Harvie [11] for the ERBS spacecraft. The Kalman filter outperformed a batch least-squares estimator in both roll and pitch, but diverged in yaw. This divergence could be reduced by proper tuning of model error covariance terms, but appropriate tuning differed for other data sets. Therefore, Chu and Harvie [11] concluded that the inconsistency in yaw behavior makes the use of the Kalman filter impractical for routine operation. This study as well as the SAMPEX study [15-16] confirm that more robust algorithms are needed to obtain optimal attitude estimates in the presence of both inaccurate models and loss or intentional omission of rate gyros.

Although the quaternion representation is the most commonly used for attitude estimation, the problem of maintaining proper normalization exists. This constraint leads to a singularity in the covariance matrix which in actual practice is difficult to maintain due to linearization and/or computer round-off error. Three solutions (two of which yield identical results) to this problem are summarized by Lefferts et al. [10]. The first approach uses the transition matrix of the state-error vector to obtain a reduced order representation of the error covariance. The second approach deletes one of the quaternion components in order to obtain a truncated error covariance expression. The third approach uses an incremental quaternion error which results in a representation that is identical to the first approach. This approach is most commonly used to maintain normalization for the estimated quaternion.

Bar-Itzhack and Deutschmann [12] show two further approaches to quaternion normalization. The first approach represents the state vector by additive corrections to the quaternion estimated by the Kalman filter. However, this approach does not maintain the normalization constraint unless it converges to the correct quaternion [12]. Re-normalization is carried out externally to the Kalman filter. This approach can be useful in obtaining a faster convergence, but lacks physical sense in the filter's state propagation. The second approach uses the normalized quaternion as a "pseudo-measurement." The re-normalization is subsequently carried out by performing a measurement update with ideally zero noise on the "pseudo-measurement," thereby forcing the estimated quaternion to the normalized quaternion. However, attitude solutions converge to incorrect values when noise levels are high in nature (see [12] for more details).

The quaternion normalization constraint is essential for true attitude representations, but is difficult to maintain when utilizing linearized equations of kinematic and dynamic models in an extended Kalman filter. In both theory and actual practice quaternion kinematic relations must always hold true. Therefore, the ideal approach to maintaining the normalization constraint is not to utilize linearized kinematic equations of motion.

In this paper, an optimal attitude estimation algorithm is developed which is capable of robust and accurate state estimation for spacecraft lacking accurate or any gyro measurements and/or accurate dynamic models. This algorithm is based on the Minimum Model Error (MME) [17] batch-estimation approach. The advantages of the MME

estimator over conventional Kalman strategies include: (i) no a priori statistics on the form of the model error are required, (ii) the actual model error is determined as part of the solution, and (iii) states estimates are free of jump discontinuities. The MME estimation approach has been successfully applied to numerous poorly-modeled dynamic systems which exhibit highly nonlinear behaviors (see, e.g. [18-19]).

The purpose of this paper is to derive a computationally efficient spacecraft attitude estimation algorithm using an MME-based approach. Initial results using an MME approach to estimate the attitude and angular rates of SAMPEX utilized TRIAD determined attitudes as measurements (see [20-21]). The formulation developed in this paper expands upon this technique to use attitude sensors, such as three-axis magnetometers (TAM), fine sun sensors (FSS), star trackers, etc. Models which either may or may not include gyro measurements in the estimator design are developed. Previously, the MME estimator problem was solved by using gradient based techniques (see [22]). However, gradient based techniques have difficulty converging near the minimum. Therefore, the MME-based estimation scheme presented in this paper also utilizes a linearization technique with a Riccati transformation. This leads to an algorithm which is easy to design and implement in actual practice.

The organization of this paper proceeds as follows. First, a summary of the spacecraft attitude kinematics and sensor models is shown. Then, a brief review of the MME estimator for nonlinear systems is shown. Next, the MME-based estimator is developed for the purpose of attitude estimation. This approach determines the optimal angular velocity by minimizing a quadratic cost function. This case also includes systems which may utilize discrete or continuous-time gyro measurements. A linearization technique is then applied in order to solve the two-point-boundary-value-problem associated with the MME estimation problem. Finally, the MME estimator is used to estimate the attitude of SAMPEX in order to demonstrate the usefulness of this algorithm.

Attitude Kinematics and Dynamics

In this section, a brief review of the kinematic and dynamic equations of motion for a three-axis stabilized spacecraft is shown. The attitude is assumed to be represented by the quaternion vector, defined as

$$\underline{q} \equiv \begin{bmatrix} \underline{q}_{13} \\ q_4 \end{bmatrix} \tag{1a}$$

with

$$\underline{q}_{13} \equiv \begin{bmatrix} q_1 \\ q_2 \\ q_3 \end{bmatrix} = \hat{\underline{n}} \sin\left(\theta/2\right), \qquad q_4 = \cos\left(\theta/2\right) \tag{1b}$$

where $\hat{\underline{n}}$ is a unit vector corresponding to the axis of rotation and θ is the angle of rotation. The quaternion kinematic equations of motion are derived by using the spacecraft's angular velocity ($\underline{\omega}$), given by

$$\dot{\underline{q}} = \frac{1}{2}\Omega\left(\underline{\omega}\right)\underline{q} = \frac{1}{2}\Xi\left(\underline{q}\right)\underline{\omega} \tag{2}$$

where $\Omega\left(\underline{\omega}\right)$ and $\Xi\left(\underline{q}\right)$ are defined as

$$\Omega\left(\underline{\omega}\right) \equiv \begin{bmatrix} -\left[\underline{\omega}\times\right] & \vdots & \underline{\omega} \\ \cdots\cdots & \vdots & \cdots\cdots \\ -\underline{\omega}^T & \vdots & 0 \end{bmatrix}, \quad \Xi\left(\underline{q}\right) \equiv \begin{bmatrix} q_4 I_{3\times 3} + \left[\underline{q}_{13}\times\right] \\ \cdots\cdots\cdots\cdots\cdots \\ -\underline{q}_{13}^T \end{bmatrix} \tag{3}$$

The 3×3 dimensional matrices $\left[\underline{\omega}\times\right]$ and $\left[\underline{q}_{13}\times\right]$ are referred to as cross product matrices since $\underline{a}\times\underline{b} = \left[\underline{a}\times\right]\underline{b}$, with

$$\left[\underline{a}\times\right] \equiv \begin{bmatrix} 0 & -a_3 & a_2 \\ a_3 & 0 & -a_1 \\ -a_2 & a_1 & 0 \end{bmatrix} \tag{4}$$

Since a three degree-of-freedom attitude system is represented by a four-dimensional vector, the quaternions cannot be independent. This condition leads to the following normalization constraint

$$\underline{q}^T\,\underline{q} = \underline{q}_{13}^T\underline{q}_{13} + q_4^2 = 1 \tag{5}$$

Also, the matrix $\Xi\left(\underline{q}\right)$ obeys the following helpful relations

$$\Xi^T\left(\underline{q}\right)\Xi\left(\underline{q}\right) = \underline{q}^T\,\underline{q}\,I_{3\times 3} \tag{6a}$$

$$\Xi\left(\underline{q}\right)\Xi^T\left(\underline{q}\right) = \underline{q}^T\,\underline{q}\,I_{4\times 4} - \underline{q}\,\underline{q}^T \tag{6b}$$

$$\Xi^T\left(\underline{q}\right)\underline{q} = \underline{0}_{3\times 1} \tag{6c}$$

$$\Xi^T\left(\underline{q}\right)\underline{\lambda} = -\Xi^T\left(\underline{\lambda}\right)\underline{q} \quad \text{for any } \underline{\lambda}_{4\times 1} \tag{6d}$$

The dynamic equations of motion, also known as Euler's equations, for a rotating spacecraft are given by ([23])

$$\dot{\underline{L}} = \underline{N} - \underline{\omega}\times\underline{L} = I_b\,\dot{\underline{\omega}} \tag{7}$$

where $\underline{L}$ is the total angular momentum, $\underline{N}$ is the total external torque (which includes, e.g., control torques, aerodynamic drag torques, solar pressure torques, etc.), and I_b is the inertia matrix of the spacecraft. If reaction or momentum wheels are used on the spacecraft, the total angular momentum is given by

$$\underline{L} = I_b\,\underline{\omega} + \underline{h} \tag{8}$$

where $\underline{h}$ is the total angular momentum due to the wheels. Thus, Equation (7) can be re-written as

$$\dot{\underline{L}} = \underline{N} - \left[I_b^{-1}\left(\underline{L} - \underline{h}\right)\right]\times\underline{L} \tag{9}$$

where all vectors are still resolved in the body-fixed coordinate system.

The measurement model is assumed to be of the form given by

$$\underline{B}_B = A\left(\underline{q}\right)\underline{B}_I \tag{10}$$

where $\underline{B}_I$ is a 3×1 dimensional vector of some reference object (e.g., a vector to the sun or to a star, or the Earth's magnetic field vector) in a reference coordinate system, $\underline{B}_B$ is a 3×1 dimensional vector defining the components of the corresponding reference vector measured in the spacecraft body frame, and $A\left(\underline{q}\right)$ is given by

$$A\left(\underline{q}\right) = \left(q_4^2 - \underline{q}_{13}^T\underline{q}_{13}\right)I_{3\times3} + 2\,\underline{q}_{13}\underline{q}_{13}^T - 2\,q_4\left[\underline{q}_{13}\times\right] \tag{11}$$

which is the 3×3 dimensional (orthogonal) attitude matrix.

Minimum Model Error Estimation

In this section, a brief review of the Minimum Model Error (MME) estimation algorithm is shown. The essential feature of this batch estimator is that actual model error trajectories are determined during the estimation process, unlike most filter/smoother algorithms which assume that the model error is a stochastic process with known properties. The MME algorithm determines the correction added to the assumed model which yields an accurate representation of the system's behavior. This is accomplished by solving an optimality condition using an output residual constraint. Therefore, accurate state estimates can be determined without the use of precise system representations in the assumed model.

The MME algorithm assumes that the state estimates are given by a preliminary model and a to-be-determined model error vector, given by

$$\dot{\hat{\underline{x}}}(t) = \underline{f}\left[\hat{\underline{x}}(t), \underline{u}(t), \underline{d}(t), t\right] \tag{12a}$$

$$\hat{\underline{y}}(t) = \underline{g}\left[\hat{\underline{x}}(t), t\right] \tag{12b}$$

where $\underline{f}$ is an $n\times1$ model vector, $\hat{\underline{x}}(t)$ is an $n\times1$ state estimate vector, $\underline{u}(t)$ is a $p\times1$ vector of known inputs, and $\underline{d}(t)$ is an $l\times1$ model error vector, $\underline{g}$ is a $q\times1$ measurement (sensitivity) vector, and $\hat{\underline{y}}(t)$ is a $q\times1$ estimated output vector. State-observable discrete measurements are assumed for Equation (12b) in the following form

$$\tilde{\underline{y}}(t_k) = \underline{g}_k\left[\underline{x}(t_k), t_k\right] + \underline{v}_k \tag{13}$$

where $\tilde{\underline{y}}(t_k)$ is a $q\times1$ measurement vector at time t_k, and $\underline{v}_k$ is a $q\times1$ measurement noise vector which is assumed to be a zero-mean, Gaussian distributed process with known covariance.

In the MME algorithm, the optimal state estimates are determined on the basis that the measurement-minus-estimate error covariance matrix must match the measurement-minus-truth error covariance matrix. This condition is referred to as the "covariance constraint," shown as

$$\left\{\tilde{\underline{y}}(t_k) - \underline{g}_k\left[\hat{\underline{x}}(t_k), t_k\right]\right\}\left\{\tilde{\underline{y}}(t_k) - \underline{g}_k\left[\hat{\underline{x}}(t_k), t_k\right]\right\}^T = R_k \tag{14}$$

where R_k is the element-by-element (known) measurement error covariance. However, problems may arise using Equation (14) which are attributed to "small sample" statistics [24]. Therefore, in the typical case where the measurement error process is stationary, the average covariance can be used, given by

$$\frac{1}{m}\sum_{k=1}^{m}\left\{\tilde{\underline{y}}(t_k) - \underline{g}_k\left[\hat{\underline{x}}(t_k), t_k\right]\right\}\left\{\tilde{\underline{y}}(t_k) - \underline{g}_k\left[\hat{\underline{x}}(t_k), t_k\right]\right\}^T \approx R \tag{15}$$

where m is the total number of measurements.

Next, the following cost function is minimized with respect to $\underline{d}(\tau)$

$$J = \frac{1}{2}\sum_{k=1}^{m}\left\{\tilde{\underline{y}}(t_k) - \underline{g}_k\left[\hat{\underline{x}}(t_k), t_k\right]\right\}^T R^{-1}\left\{\tilde{\underline{y}}(t_k) - \underline{g}_k\left[\hat{\underline{x}}(t_k), t_k\right]\right\} + \frac{1}{2}\int_{t_0}^{t_f}\underline{d}^T(\tau)\,W\,\underline{d}(\tau)\,d\tau \tag{16}$$

where W is an $n\times n$ positive-definite weighting matrix. The necessary conditions for the minimization of J lead to the following two-point-boundary-value-problem (TPBVP) [17]

$$\dot{\hat{\underline{x}}}(t) = \underline{f}\left[\hat{\underline{x}}(t), \underline{u}(t), \underline{d}(t), t\right] \tag{17a}$$

$$\underline{d}(t) = -W^{-1}\left[\frac{\partial \underline{f}}{\partial \underline{d}}\right]^T \underline{\lambda}(t) \tag{17b}$$

$$\dot{\underline{\lambda}}(t) = -\left[\frac{\partial \underline{f}}{\partial \hat{\underline{x}}}\right]^T \underline{\lambda}(t) \tag{17c}$$

$$\underline{\lambda}\left(t_k^+\right) = \underline{\lambda}\left(t_k^-\right) + H^T(t_k)\left\{\tilde{\underline{y}}(t_k) - \underline{g}_k\left[\hat{\underline{x}}(t_k), t_k\right]\right\}$$
$$H(t_k) \equiv \left.\frac{\partial \underline{g}}{\partial \hat{\underline{x}}}\right|_{\hat{\underline{x}}(t_k), t_k} \tag{17d}$$

where $\underline{\lambda}(t)$ is an $n\times1$ co-state vector which is updated at each measurement point using Equation (17d). The boundary conditions are selected such that either $\underline{\lambda}\left(t_0^-\right) = \underline{0}$ or $\hat{\underline{x}}(t_0)$ is specified at the initial time and either $\underline{\lambda}\left(t_f^+\right) = \underline{0}$ or $\hat{\underline{x}}\left(t_f\right)$ is specified at the final time.

The solution of the TPBVP for a given weighting matrix yields a state estimate time trajectory which can be used to determine a measurement residual covariance matrix. The covariance constraint is satisfied when the proper balance between model error and measurement residual has been achieved. If the measurement residual covariance is higher than the known measurement error covariance (R), then W

should be decreased to less penalize the model error. Conversely, if the residual covariance is lower than the known covariance, then W should be increased so that less unmodeled dynamics are added to the assumed system model. The optimal weighting matrix is therefore obtained when the covariance constraint in Equation (15) is satisfied.

Attitude Estimation

In this section, the MME estimator is formulated for attitude estimation using attitude sensors and/or gyro measurements. First, an MME-based algorithm is shown which smoothes noisy gyro measurements. Then, a fourth-order MME estimation scheme is derived to estimate angular velocities with or without gyro measurements. Finally, a seventh order model is used to estimate angular accelerations, which provides smoother angular velocity estimates.

Gyro Noise Smoother

Gyros tend to be very noisy and have an inherent drift. Also, gyros are usually sampled at a higher frequency than attitude sensors. In order to first filter the noise, a simple MME-based smoothing algorithm can first be applied. This algorithm minimizes

$$J_g = \frac{1}{2}\sum_{k=1}^{m}\left\{\tilde{\underline{\omega}}_{g_k} - \hat{\underline{\omega}}_{g_k}\right\}^T R_g^{-1}\left\{\tilde{\underline{\omega}}_{g_k} - \hat{\underline{\omega}}_{g_k}\right\} + \frac{1}{2}\int_{t_0}^{t_f} \underline{d}_g^T(\tau)\, W_g\, \underline{d}_g(\tau)\, d\tau \tag{18}$$

subject to

$$\dot{\hat{\underline{\omega}}}_g(t) = \underline{d}_g(t), \qquad \hat{\underline{\omega}}_g(t_0) = \hat{\underline{\omega}}_{g0} \tag{19}$$

where $\hat{\underline{\omega}}_g$ is the estimated gyro output, and $\underline{d}_g$ is the model error correction. Minimizing Equation (18) leads to

$$\dot{\hat{\underline{\omega}}}_g(t) = -W_g^{-1}\underline{\lambda}_g(t), \qquad \hat{\underline{\omega}}_g(t_0) = \hat{\underline{\omega}}_{g0} \tag{20a}$$

$$\dot{\underline{\lambda}}_g = \underline{0} \tag{20b}$$

$$\underline{\lambda}_g\left(t_k^+\right) = \underline{\lambda}_g\left(t_k^-\right) + R_g^{-1}\left\{\tilde{\underline{\omega}}_{g_k} - \hat{\underline{\omega}}_{g_k}\right\}, \quad \underline{\lambda}_g\left(t_f^-\right) = \underline{0} \tag{20c}$$

The solution of Equation (20) can be determined by using a steady-state Riccati transformation (see [25] for details). This transformation leads to the following

$$P_i = \sqrt{\frac{W_{g_i}}{R_{g_i}\Delta t}} \tag{21a}$$

$$\dot{\underline{h}}_i(t) = \left[\frac{P_i}{W_{g_i}}\right]\underline{h}_i(t) \tag{21b}$$

$$\underline{h}_i\left(t_k^-\right) = \underline{h}_i\left(t_k^+\right) - \frac{1}{R_{g_i}}\tilde{\underline{\omega}}_{g_i}(t_k), \quad \underline{h}_i\left(t_f^+\right) = \underline{0} \tag{21c}$$

$$\dot{\hat{\underline{\omega}}}_{g_i}(t) = \left[\frac{P_i}{W_{g_i}}\right]\hat{\underline{\omega}}_{g_i}(t) - \left[\frac{1}{W_{g_i}}\right]\underline{h}_i(t), \quad \hat{\underline{\omega}}_{g_i}(t_0) = \hat{\underline{\omega}}_{gi_0} \tag{21d}$$

where the subscript (i) represents each gyro measurement set, and Δt is the sampling interval. For a given weighting and measurement covariance, the first step is to determine the steady-state Riccati solution in using Equation (21a). Then, the inhomogeneous Riccati trajectory is solved backwards in time using Equation (21b), with discrete jumps at each measurement point given by Equation (21c). Finally, the smoothed gyro estimates are determined using Equation (21d). An advantage of the MME algorithm is not only the inherent smoothing properties, but also that the gyro estimates are totally continuous. Therefore, the generally discrete gyro measurements can be replaced with the continuous gyro estimates given by Equation (21d).

Angular Velocity Estimation

The MME attitude angular velocity estimation formulation minimizes the following cost function

$$J = \frac{1}{2}\sum_{k=1}^{m}\left\{\tilde{\underline{B}}_B - A\left(\hat{\underline{q}}\right)\underline{B}_I\right\}^T\Big|_{t_k} R^{-1}\left\{\tilde{\underline{B}}_B - A\left(\hat{\underline{q}}\right)\underline{B}_I\right\}\Big|_{t_k} + \frac{1}{2}\int_{t_0}^{t_f}\underline{d}^T(\tau)\, W\, \underline{d}(\tau)\, d\tau \tag{22}$$

subject to

$$\dot{\hat{\underline{q}}}(t) = \frac{1}{2}\Omega\left[\tilde{\underline{\omega}}_g(t) + \underline{d}(t)\right]\hat{\underline{q}}(t), \qquad \hat{\underline{q}}(t_0) = \hat{\underline{q}}_0 \tag{23}$$

where $\tilde{\underline{\omega}}_g$ is the gyro measurement vector, $\hat{\underline{q}}$ is the estimated quaternion, and $\tilde{\underline{B}}_B$ and $\underline{B}_I$ are the spacecraft body measurement and corresponding inertial field vector, respectively. The model error ($\underline{d}$) is a correction to the gyro measurements, or is equivalent to the determined angular velocity when there are no gyro measurements available.

The TPBVP given by Equation (17) can be written as

$$\dot{\hat{\underline{q}}}(t) = \frac{1}{2}\Omega\left[\tilde{\underline{\omega}}_g(t) + \underline{d}(t)\right]\hat{\underline{q}}(t), \qquad \hat{\underline{q}}(t_0) = \hat{\underline{q}}_0 \tag{24a}$$

$$\underline{d}(t) + \frac{1}{2}W^{-1}\Xi^T\left(\hat{\underline{q}}\right)\underline{\lambda}(t) = 0 \tag{24b}$$

$$\dot{\underline{\lambda}}(t) = \frac{1}{2}\Omega\left[\tilde{\underline{\omega}}_g(t) + \underline{d}(t)\right]\underline{\lambda}(t) \tag{24c}$$

$$\underline{\lambda}\left(t_k^+\right) = \underline{\lambda}\left(t_k^-\right) + H^T\Big|_{t_k} R^{-1}\left\{\tilde{\underline{B}}_B - A\left(\hat{\underline{q}}\right)\underline{B}_I\right\}\Big|_{t_k}, \quad \underline{\lambda}\left(t_f^+\right) = \underline{0} \tag{24d}$$

The sensitivity matrix H in Equation (24d) can be derived as

$$H = 2\Xi^T\left(\underline{h}\right) \tag{25}$$

where

$$\underline{h} = \Psi\left(\hat{\underline{q}}\right)\underline{B}_I \tag{26a}$$

$$\Psi\left(\hat{\underline{q}}\right) \equiv \begin{bmatrix} -\hat{q}_4 I_{3\times 3} + \left[\hat{\underline{q}}_{13}\times\right] \\ \cdots\cdots\cdots\cdots\cdots \\ \hat{\underline{q}}_{13}^T \end{bmatrix} \tag{26b}$$

The extension to using multiple attitude sensors is accomplished by using a partitioned residual output and sensitivity matrix, given by

$$\begin{bmatrix} H_1^T & \cdots & H_q^T \end{bmatrix} \begin{bmatrix} \left\{\tilde{\underline{B}}_{B_1} - A\left(\hat{\underline{q}}\right)\underline{B}_{I_1}\right\} \\ \vdots \\ \left\{\tilde{\underline{B}}_{B_q} - A\left(\hat{\underline{q}}\right)\underline{B}_{I_q}\right\} \end{bmatrix} \tag{27}$$

The co-state update in Equation (24d) shows a nonlinear relationship with respect to the quaternion estimate. However, this nonlinearity can be reduced to be a *linear* function if the quaternions obey normalization and each attitude sensor is assumed isotropic. This can be shown by deriving the co-state update using

$$\frac{1}{2r}\frac{\partial}{\partial \hat{\underline{q}}}\left\{\left[\tilde{\underline{B}}_B - A\left(\hat{\underline{q}}\right)\underline{B}_I\right]^T\left[\tilde{\underline{B}}_B - A\left(\hat{\underline{q}}\right)\underline{B}_I\right]\right\} \tag{28}$$

where the measurement covariance is now assumed to be isotropic for each sensor (i.e., the measurement errors in each one of the axes are assumed equal). Therefore, $R = rI_{3\times 3}$, which is a valid assumption for most all attitude sensors. In order to determine the partial derivative in Equation (28), the following identities and definitions are used

$$\mathrm{E}\left(\underline{B}_I\right) \equiv \begin{bmatrix} -\left[\underline{B}_I\times\right] & \vdots & -\underline{B}_I \\ \cdots\cdots & \vdots & \cdots\cdots \\ \underline{B}_I^T & \vdots & 0 \end{bmatrix} \tag{29a}$$

$$A\left(\hat{\underline{q}}\right) = -\Xi^T\left(\hat{\underline{q}}\right)\Psi\left(\hat{\underline{q}}\right) \tag{29b}$$

$$\Psi\left(\hat{\underline{q}}\right)\underline{B}_I = \mathrm{E}\left(\underline{B}_I\right)\hat{\underline{q}} \tag{29c}$$

$$\mathrm{E}^2\left(\underline{B}_I\right) = -I_{4\times 4}\underline{B}_I^T\underline{B}_I \tag{29d}$$

Equation (28) can now be re-written as

$$\frac{1}{2r}\frac{\partial}{\partial \hat{\underline{q}}}\left\{\tilde{\underline{B}}_B^T\tilde{\underline{B}}_B - 2\hat{\underline{q}}^T\Omega\left(\tilde{\underline{B}}_B\right)\mathrm{E}\left(\underline{B}_I\right)\hat{\underline{q}} + I_{4\times 4}\left(\underline{B}_I^T\underline{B}_I\right)\left(\hat{\underline{q}}^T\hat{\underline{q}}\right)^2\right\} \tag{30}$$

The partial derivative in Equation (29) is given by

$$\frac{2}{r}\left\{\Omega\left(\tilde{\underline{B}}_B\right)\mathrm{E}\left(\underline{B}_I\right)\hat{\underline{q}} + \left(\underline{B}_I^T\underline{B}_I\right)\left(\hat{\underline{q}}^T\hat{\underline{q}}\right)\hat{\underline{q}}\right\} \tag{31}$$

If the quaternions obey normalization, then the following identity is true

$$\left\{\Omega\left(\tilde{\underline{B}}_B\right)\mathrm{E}\left(\underline{B}_I\right)\hat{\underline{q}} + \left(\underline{B}_I^T\underline{B}_I\right)\hat{\underline{q}}\right\} = \Xi\left(\underline{h}\right)\left\{\tilde{\underline{B}}_B - A\left(\hat{\underline{q}}\right)\underline{B}_I\right\} \tag{32}$$

Therefore, the co-state update in Equation (24d) is linear with respect to the quaternion estimate. This relationship is useful for developing a linearized MME algorithm.

The TPBVP shown in Equations (24a)-(24d) can be solved by using gradient techniques. The basic gradient procedure is to first guess for the model error trajectory ($\underline{d}$). Then, integrate the quaternion states forward using Equation (24a) and co-states backward using Equation (24c) accounting for discrete jumps in Equation (24d). The next search direction is given by Equation (24b). This procedure is continued until convergence is achieved. However, experience has shown that the gradient search technique has difficulty converging near the minimum [22]. Conjugate gradient techniques can help the solution to converge. However, a different approach is used to achieve a fast convergence near the minimum. This involves linearizing the state and co-state equations by using error quaternion multiplication (this approach is similar to the linear equations used in [10]). First, define an error quaternion given by

$$\delta\hat{\underline{q}} = \hat{\underline{q}} \otimes \underline{q}_n^{-1} \tag{33}$$

where $\delta\hat{\underline{q}}$ is the error quaternion and $\underline{q}_n$ is a nominal quaternion determined by the gradient search technique. The inverse quaternion is determined by taking the negative of the first three components. The quaternion product is defined as

$$\underline{q}_a \otimes \underline{q}_b \equiv \left[\Xi\left(\underline{q}_b\right) \;\vdots\; \underline{q}_b\right]\underline{q}_a \tag{34}$$

Taking the time derivative of Equation (33) yields

$$\delta\dot{\hat{\underline{q}}} = \dot{\hat{\underline{q}}} \otimes \underline{q}_n^{-1} + \hat{\underline{q}} \otimes \dot{\underline{q}}_n^{-1} \tag{35}$$

Substituting the quaternion kinematic equations into Equation (35) gives

$$\delta\dot{\hat{\underline{q}}} = \frac{1}{2}\begin{bmatrix}\underline{d} \\ 0\end{bmatrix} \otimes \delta\hat{\underline{q}} - \frac{1}{2}\delta\hat{\underline{q}} \otimes \begin{bmatrix}\underline{d}_n \\ 0\end{bmatrix} \tag{36}$$

where $\underline{d}_n$ is the nominal model error determined by the gradient search. Equation (36) can be re-written as

$$\delta\dot{\hat{\underline{q}}} = \frac{1}{2}\left\{\begin{bmatrix}\underline{d}_n \\ 0\end{bmatrix} \otimes \delta\hat{\underline{q}} - \delta\hat{\underline{q}} \otimes \begin{bmatrix}\underline{d}_n \\ 0\end{bmatrix}\right\} + \frac{1}{2}\begin{bmatrix}\delta\underline{d} \\ 0\end{bmatrix} \otimes \delta\hat{\underline{q}} \tag{37}$$

where

$$\delta\underline{d} = \underline{d} - \underline{d}_n \tag{38}$$

If $\delta\hat{\underline{q}}_4 \approx 1$ then second order terms in Equation (37) are negligible and the fourth derivative error component is zero, which leads to

$$\delta\dot{\hat{\underline{q}}}_{13} = -\left[\underline{d}_n\times\right]\delta\hat{\underline{q}}_{13} + \frac{1}{2}\delta\underline{d} \tag{39}$$

with

$$\delta\hat{\underline{q}}_{13} = \Xi^T\left(\underline{q}_n\right)\hat{\underline{q}} \tag{40}$$

In order to determine $\delta\underline{d}$ the cost function in Equation (22) is minimized subject to the equality constraint in Equation (39). This minimization leads to the following TPBVP

$$\delta\dot{\hat{\underline{q}}}_{13} = -\left[\underline{d}_n\times\right]\delta\hat{\underline{q}}_{13} - \frac{1}{2}\underline{d}_n - \frac{1}{4}W^{-1}\underline{\lambda} \tag{41a}$$

$$\dot{\underline{\lambda}} = -\left[\underline{d}_n\times\right]\underline{\lambda} \tag{41b}$$

$$\underline{\lambda}\left(t_k^+\right) = \underline{\lambda}\left(t_k^-\right) + H^T\Big|_{t_k}\frac{1}{r}\left\{\tilde{\underline{B}}_B - A\left(\underline{q}_n\right)\underline{B}_I - H\,\delta\hat{\underline{q}}_{13}\right\}\Big|_{t_k} \tag{41c}$$

$$H = 2\left[A\left(\underline{q}_n\right)\underline{B}_I\times\right] \tag{41d}$$

where the following equation is used to derive the co-state update in Equation (41c) [10]

$$A\left(\delta\hat{\underline{q}}\right) = I_{3\times3} - 2\left[\delta\hat{\underline{q}}_{13}\times\right] \tag{42}$$

The boundary conditions for the TPBVP are selected as $\delta\hat{\underline{q}}_{13}\left(t_0\right) = \underline{0}$ and $\underline{\lambda}\left(t_f^+\right) = \underline{0}$.

The TPBVP in Equation (41) can be decoupled by introducing a time-varying Riccati transformation (see [25]). This leads to the following set of equations

$$\dot{P} = P\left[\underline{d}_n\times\right] + \left[\underline{d}_n\times\right]^T P + \frac{1}{4}PW^{-1}P \tag{43a}$$

$$P\left(t_k^-\right) = P\left(t_k^+\right) - \frac{4}{r}\left[A\left(\underline{q}_n\right)\underline{B}_I\times\right]^2\Big|_{t_k}, \quad P\left(t_f^+\right) = 0 \tag{43b}$$

$$\dot{\underline{h}} = \left\{\frac{1}{4}PW^{-1} - \left[\underline{d}_n\times\right]\right\}\underline{h} + \frac{1}{2}P\underline{d}_n \tag{43c}$$

$$\underline{h}\left(t_k^-\right) = \underline{h}\left(t_k^+\right) + \frac{2}{r}\left[A\left(\underline{q}_n\right)\underline{B}_I\times\right]\tilde{\underline{B}}_B\Big|_{t_k}, \quad \underline{h}\left(t_f^+\right) = \underline{0} \tag{43d}$$

Therefore, the Riccati trajectories in Equation (43a) are integrated backwards in time with discrete updates given at the measurement time by Equation (43b). Then, the inhomogeneous trajectories in Equation (43c) are integrated backwards in time accounting for discrete jumps using Equation (43d). Finally, the error quaternion trajectories can be solved by integrating the following equation forward in time

$$\delta\dot{\hat{\underline{q}}}_{13} = -\left\{\left[\underline{d}_n\times\right] + \frac{1}{4}W^{-1}P\right\}\delta\hat{\underline{q}}_{13} - \frac{1}{2}\underline{d}_n - \frac{1}{4}W^{-1}\underline{h} \tag{44}$$

and the estimated quaternion trajectories can then be constructed by using

$$\hat{\underline{q}} = \begin{bmatrix}\delta\hat{\underline{q}}_{13}\\ 1\end{bmatrix}\otimes\underline{q}_n \tag{45}$$

The linearized approach shown here converges in one step if the nominal quaternion estimate (determined from a gradient search) is *close* to the final solution. However, the linearized approach may be repeated until a satisfactory solution is determined.

Angular Acceleration Estimation

In this section the angular acceleration of a spacecraft is estimated using an MME approach. This has the advantage of further refining the angular velocity estimates. The cost function used is identical to Equation (22), subject to

$$\begin{bmatrix}\dot{\hat{\underline{q}}}\\ \dot{\hat{\underline{b}}}\end{bmatrix} = \begin{bmatrix}\frac{1}{2}\Omega\left(\tilde{\underline{\omega}}_g + \hat{\underline{b}}\right) & 0_{4\times3}\\ 0_{3\times4} & 0_{3\times3}\end{bmatrix}\begin{bmatrix}\hat{\underline{q}}\\ \hat{\underline{b}}\end{bmatrix} + \begin{bmatrix}0_{4\times3}\\ I_{3\times3}\end{bmatrix}\underline{d}, \qquad \begin{bmatrix}\hat{\underline{q}}\left(t_0\right)\\ \hat{\underline{b}}\left(t_0\right)\end{bmatrix} = \begin{bmatrix}\hat{\underline{q}}_0\\ \hat{\underline{b}}_0\end{bmatrix} \tag{46}$$

The initial condition for the estimated rate $\underline{b}_0$ is assumed known in this formulation. This can be determined by using a finite difference of the initial attitude matrix (see [16]). Minimizing the cost function in Equation (22) subject to Equation (46) leads to the following equations for the model error and co-states

$$W\underline{d} + \underline{\lambda}_b = \underline{0} \tag{47a}$$

$$\begin{bmatrix}\dot{\underline{\lambda}}_q\\ \dot{\underline{\lambda}}_b\end{bmatrix} = \begin{bmatrix}\frac{1}{2}\Omega\left(\tilde{\underline{\omega}}_g + \hat{\underline{b}}\right) & 0_{4\times3}\\ -\Xi^T\left(\hat{\underline{q}}\right) & 0_{3\times3}\end{bmatrix}\begin{bmatrix}\underline{\lambda}_q\\ \underline{\lambda}_b\end{bmatrix} \tag{47b}$$

$$\underline{\lambda}_q\left(t_k^+\right) = \underline{\lambda}_q\left(t_k^-\right) + H^T\Big|_{t_k}R^{-1}\left\{\tilde{\underline{B}}_B - A\left(\hat{\underline{q}}\right)\underline{B}_I\right\}\Big|_{t_k}, \qquad \underline{\lambda}_q\left(t_f^+\right) = \underline{0},\ \underline{\lambda}_b\left(t_f\right) = \underline{0} \tag{47c}$$

A linearized set of equations can again be used to achieve a fast convergence near the minimum. The state equation used for the linearized equation is given by

$$\dot{\hat{\underline{x}}} = A\hat{\underline{x}} - \frac{1}{2}D_1\underline{d}_n + D_2\underline{d}, \quad \hat{\underline{x}}\left(t_0\right) = \hat{\underline{x}}_0 = \begin{bmatrix}\underline{0}\\ \underline{b}_0\end{bmatrix} \tag{48}$$

where

$$\hat{\underline{x}} = \begin{bmatrix}\delta\hat{\underline{q}}_{13}\\ \hat{\underline{b}}\end{bmatrix} \tag{49a}$$

$$A = \begin{bmatrix}-\left[\underline{d}_n\times\right] & \frac{1}{2}I_{3\times3}\\ 0_{3\times3} & 0_{3\times3}\end{bmatrix} \tag{49b}$$

$$D_1 = \begin{bmatrix}I_{3\times3}\\ 0_{3\times3}\end{bmatrix}, \qquad D_2 = \begin{bmatrix}0_{3\times3}\\ I_{3\times3}\end{bmatrix} \tag{49c}$$

Applying a Riccati transformation similar to the previous section leads to the following set of equations

$$\dot{P} = -P\,A - A^T P + P\,D_2 W^{-1} D_2^T P \tag{50a}$$

$$P\left(t_k^-\right) = P\left(t_k^+\right) - \frac{4}{r} D_1 \left[A\left(\underline{q}_n\right) \underline{B}_I \times \right]^2 D_1^T \Big|_{t_k} \quad , \quad P\left(t_f^+\right) = 0 \tag{50b}$$

$$\dot{\underline{h}} = \left\{ P D_2 W^{-1} D_2^T - A^T \right\} \underline{h} + \frac{1}{2} P\, D_1 \underline{d}_n \tag{50c}$$

$$\underline{h}\left(t_k^-\right) = \underline{h}\left(t_k^+\right) + \frac{2}{r} D_1 \left[A\left(\underline{q}_n\right) \underline{B}_I \times \right] \tilde{\underline{B}}_B \Big|_{t_k} \quad , \quad \underline{h}\left(t_f^+\right) = \underline{0} \tag{50d}$$

$$\dot{\hat{\underline{x}}} = \left\{ A - D_2 W^{-1} D_2^T P \right\} \hat{\underline{x}} - \frac{1}{2} D_1 \underline{d}_n - D_2 W^{-1} D_2^T \underline{h} \qquad \hat{\underline{x}}\left(t_0\right) = \hat{\underline{x}}_0 \tag{49e}$$

which are solved as shown in the previous section.

Attitude Estimation of an Actual Spacecraft

In this section, the MME attitude estimation algorithm previously developed is used to estimate the attitude and rates of the SAMPEX spacecraft using magnetometer data only. The SAMPEX general mission is to study energetic particles and various types of rays. The spacecraft is three-axis stabilized in a 550 by 675 km elliptical orbit with an 82° inclination. The attitude control hardware consists of a magnetic torquer assembly (MTA) and a single reaction wheel. The attitude determination hardware consists of five coarse Sun sensors (CSS) (primarily for Sun-acquisition), one fine Sun sensor (FSS), and a three-axis magnetometer (TAM). Also, no rate gyroscopic instruments are present on the spacecraft.

The onboard computer routine to determine attitude is based upon the TRIAD [1] deterministic method. The spacecraft is controlled by the MTA to maintain the fixed solar arrays perpendicular to the sun-line. The reaction wheel is used to point the instrument boresight axis as required by the scientific mission. During eclipse no sun measurements are available from the FSS. Attitude control is maintained by using a constant sun-line vector as a "pseudo-measurement," with the use of the reaction wheel only. During vector co-alignment, the spacecraft is placed in a "coast" mode in which neither the MTA nor reaction wheel is used (see [26]). The required nominal attitude determination accuracy is ±2°. During anomalous conditions (eclipse and/or measurement co-alignment) an accuarate attitude cannot be determined by deterministic methods such as TRIAD. The MME algorithm presented here can determine the attitude using TAM measurements only, so that attitude accuracy may be checked for any deviations from nominal performance.

A plot of the magnetic field measurements from the TAM is shown in Figure 1. The inertial field trajectories are obtained by using a 8th order spherical harmonic model of the Earth's magnetic field with International Geomagnetic Reference Field (IGRF) coefficients. Magnetometer measurements by the TAM are known to be extremely accurate (within 0.3mG). However, experience has shown that errors in the magnetic field model have a standard deviation of about 3mG [16]. Therefore, 9mG is chosen for the diagonal elements of the measurement covariance matrix.

The first step for estimating the angular rates which match the TAM measurements is to run the angular velocity MME estimator to determine initial conditions. The weighting matrix is determined by using a simple parameter optimization scheme with a quadratic form of the covariance constraint as a cost function. The MME-gradient search is run for 10 iterations and then the linearized (angular velocity estimator) is run only once. Using these estimated angular velocities as nominal starting trajectories, the linearized angular acceleration MME estimator is next run once. A plot of the residuals between the estimated and measured TAM trajectories in the body frame is shown in Figure 2. This plot shows a standard deviation of about 3mG, which satisfies the covariance constraint. Plots of the finalized angular velocity and acceleration estimates are shown in Figure 3 and 4, respectively. The angular velocity estimates clearly show a rotation about the spacecraft y-axis, which is the desired control motion. Also, a plot of the attitude estimates in the GCI coordinate frame is shown in Figure 5. A plot of the error between the estimated MME attitudes and the attitudes determined by TRIAD is shown in Figure 6. A slight hangoff is seen in the pitch axis. This may be due to nonlinear effects in the magnetic field model (this hangoff is also seen in Kalman filter approaches for other spacecraft such as UARS). However, the MME algorithm is able to determine attitudes to within 0.3° using TAM data only. This can be useful in determining the attitude when deterministic methods fail.

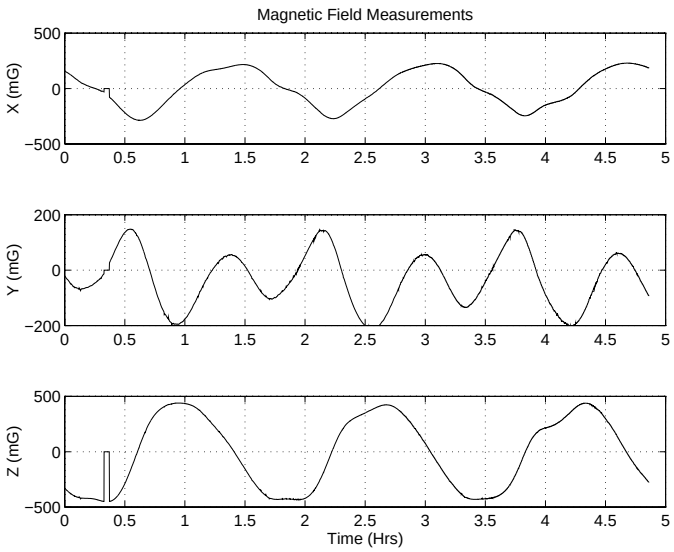

Figure 1 Plot of TAM Magnetic Field Measurements

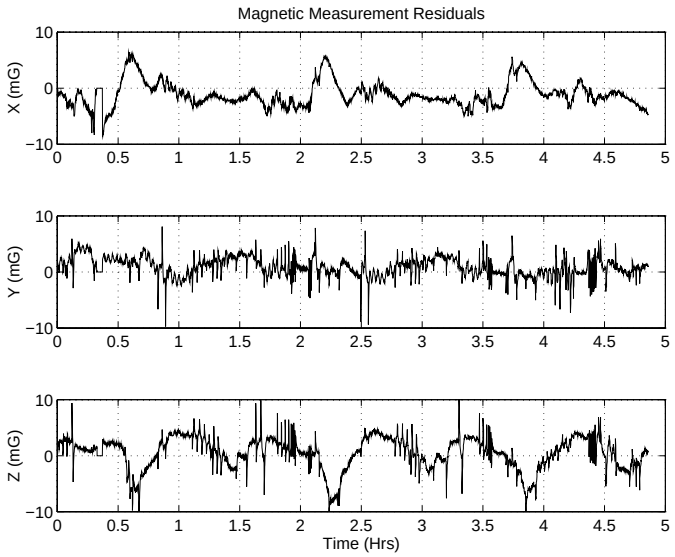

Figure 2 Plot of Estimated and Measured Residuals

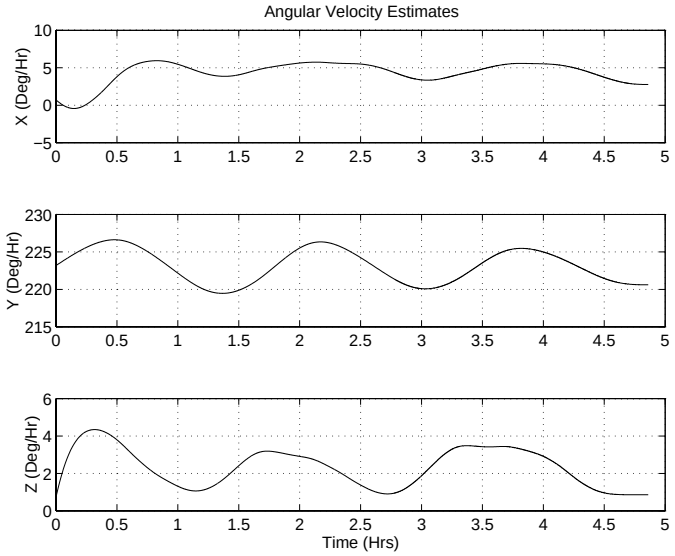

Figure 3 Plot of MME Angular Velocity Estimates

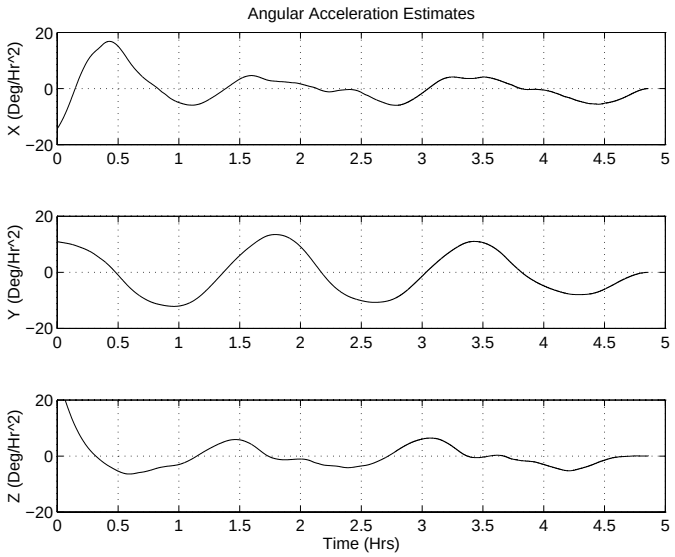

Figure 4 Plot of MME Angular Acceleration Estimates

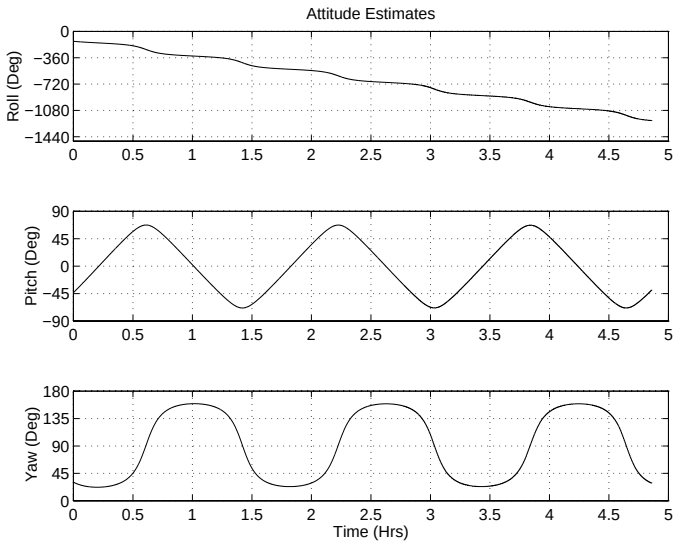

Figure 5 Plot of MME Attitude Estimates

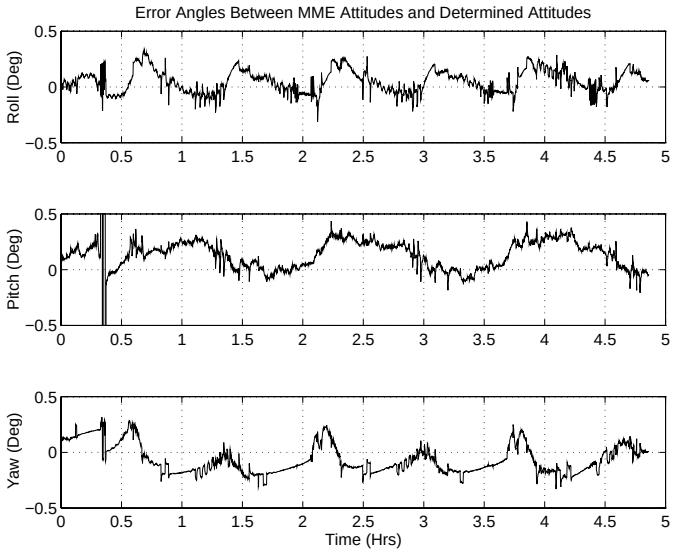

Figure 6 Plot of Attitude Errors Between TRIAD and MME

Conclusions

In this paper, a Minimum Model Error algorithm was presented for use in attitude estimation. This algorithm was developed for spacecraft which may or may not utilize angular rate sensing equipment. Two approaches were shown; one which estimates the angular velocity directly and one which estimates the angular acceleration. The first approach is useful for determining initial angular velocity estimates, while the second refines the estimation process. Linearized techniques were also developed for the two cases. These techniques help the solution converge faster near the minimum of the MME cost function. The MME-based attitude estimator was then applied to determine the dynamics of an actual spacecraft. Results indicated that an MME-based approach provides a robust algorithm which can be used to determine the attitude of a spacecraft from magnetometer measurements only.

Acknowledgments

The first author's work is supported by a National Research Council Postdoctoral Fellowship tenured at NASA-Goddard Space Flight Center. The author greatly appreciates this support. Also, this author wishes to thank D. Joseph Mook for many the comments and suggestions made throughout this work.

References

[1] Lerner, G.M., "Three-Axis Attitude Determination," *Spacecraft Attitude Determination and Control*, edited by J.R. Wertz, D. Reidel Publishing Co., Dordrecht, The Netherlands, 1978, pp. 420-428.

[2] Shuster, M.D., and Oh, S.D., "Attitude Determination from Vector Observations," *Journal of Guidance and Control*, Vol. 4, No. 1, Jan.-Feb. 1981, pp. 70-77.

[3] Markley, F.L., "Attitude Determination from Vector Observations: A Fast Optimal Matrix Algorithm," *The Journal of the Astronautical Sciences*, Vol. 41, No. 2, April-June 1993, pp. 261-280.

[4] Wahba, G., "A Least-Squares Estimate of Satellite Attitude," Problem 65-1, *SIAM Review*, Vol. 7, No. 3, July 1965, pg. 409.

[5] Kalman, R.E., "A New Approach to Linear Filtering and Prediction Problems," *Transactions of the ASME, Journal of Basic Engineering*, Vol. 82, March 1962, pp. 34-45.

[6] Gelb, A., *Applied Optimal Estimation*, MIT Press, Cambridge, Mass., 1974.

[7] Pauling, D.C., Jackson, D.B., and Brown, C.D., "SPARS Algorithms and Simulation Results," *Proceedings of the Symposium on Spacecraft Attitude Determination*, Aerospace Corp., Report TR-0066(5306)-12, Vol. 1, Sept.-Oct. 1969, pp. 293-317.

[8] Toda, N.F., Heiss, J.L., and Schlee, F.H., "SPARS:The System, Algorithms, and Test Results," *Proceedings of the Symposium on Spacecraft Attitude Determination*, Aerospace Corp., Report TR-0066(5306)-12, Vol. 1, Sept.-Oct. 1969, pp. 361-370.

[9] Shuster, M.D., "A Survey of Attitude Representations," *The Journal of the Astronautical Sciences*, Vol. 41, No. 4, Oct.-Dec. 1993, pp. 439-517.

[10] Lefferts, E.J., Markley, F.L., and Shuster, M.D., "Kalman Filtering for Spacecraft Attitude Estimation," *Journal of Guidance, Control and Dynamics*, Vol. 5, No. 5, Sept.-Oct. 1982, pp. 417-429.

[11] Chu, D., and Harvie, E., "Accuracy of the ERBS Definitive Attitude Determination System in the Presence of Propagation Noise," *Proceedings of the Flight Mechanics/Estimation Theory Symposium*, NASA-Goddard Space Flight Center, Greenbelt, MD, 1990, pp. 97-114.

[12] Bar-Itzhack, I.Y., and Deutschmann, J.K., "Extended Kalman Filter for Attitude Estimation of the Earth Radiation Budget Satellite," *Proceedings of the AAS Astrodynamics Conference*, Portland, OR, August 1990, AAS Paper #90-2964, pp. 786-796.

[13] Garrick, J., "Upper Atmospheric Research Satellite (UARS) Onboard Attitude Determination Using a Kalman Filter," *Proceedings of the Flight Mechanics/Estimation Theory Symposium*, NASA-Goddard Space Flight Center, Greenbelt, MD, 1992, pp. 471-481.

[14] Sedlack, J., "Comparison of Kalman Filter and Optimal Smoother Estimates of Spacecraft Attitude," *Proceedings of the Flight Mechanics/Estimation Theory Symposium*, NASA-Goddard Space Flight Center, Greenbelt, MD, 1992, pp. 431-445.

[15] Challa, M.S., Natanson, G.A., Baker, D.E., and Deutschmann, J.K., "Advantages of Estimating Rate Corrections During Dynamic Propagation of Spacecraft Rates-Applications to Real-Time Attitude Determination of SAMPEX," *Proceedings of the Flight Mechanics/Estimation Theory Symposium*, NASA-Goddard Space Flight Center, Greenbelt, MD, 1994, pp. 481-495.

[16] Challa, M.S*., Solar, Anomalous, and Magnetospheric Particle Explorer (SAMPEX) Real-Time Sequential Filter (RTSF)*, Evaluation Report, NASA-Goddard Space Flight Center, Greenbelt, MD, April 1993.

[17] Mook, D.J., and Junkins, J.L., "Minimum Model Error Estimation for Poorly Modeled Dynamic Systems," *Journal of Guidance, Control and Dynamics*, Vol. 3, No. 4, Jan.-Feb. 1988, pp. 367-375.

[18] Stry, G.I., and Mook, D.J., "An Analog Experimental Study of Nonlinear Identification," *Nonlinear Dynamics*, Vol. 3, No. 1, pp. 1-11.

[19] McPartland, M.D., and Mook, D.J., "Nonlinear Model Identification of Electrically Stimulated Muscle," *Proceedings of the IFAC Symposium on Modeling and Control in Biomedical Engineering*, Galveston, TX, March 1994, pp. 23-24.

[20] Mook, D.J., "Robust Attitude Determination Without Rate Gyros," *Proceedings of the AAS/GSFC International Symposium on Space Flight Dynamics*, NASA-Goddard Space Flight Center, Greenbelt, MD, April 1993, AAS Paper #93-299.

[21] DePena, J., Crassidis, J.L., McPartland, M.D., Meyer, T.J., and Mook, D.J., "MME-Based Attitude Dynamics Identification and Estimation for SAMPEX," *Proceedings of the Flight Mechanics/Estimation Theory Symposium*, NASA-Goddard Space Flight Center, Greenbelt, MD, 1994, pp. 497-512.

[22] Crassidis, J.L., and Markley, F.L., "An MME-Based Attitude Estimator Using Vector Observations," to appear in the *Flight Mechanics/Estimation Theory Symposium*, NASA-Goddard Space Flight Center, Greenbelt, MD, 1995.